Optical injection modulation of quantum-dash semiconductor lasers by intra-cavity stimulated Raman scattering

C. Chen[1,*], G. Ding[1], B. S. Ooi[1], L. F. Lester[2], A. Helmy[3], T. L. Koch[1], J. C. M. Hwang[1]

[1] *Center for Optical Technologies, Lehigh University, Bethlehem, PA 18015, USA*
[2] *Center for High Technology Materials, University of New Mexico, Albuquerque, NM 87106, USA*
[3] *Department of Electrical and Computer Engineering, University of Toronto, Toronto, ON M5S 3G4, Canada*
**chc605@lehigh.edu*

Abstract: We report the optical injection modulation of semiconductor lasers by intra-cavity stimulated Raman scattering. This mechanism manifests itself as sharply enhanced modulation bandwidth in InAs/InGaAlAs/InP quantum-dash lasers when the injected photons are 33 ± 3 meV more energetic than the lasing photons. Raman scattering measurements on the quantum-dash structure and rate equation models strongly support direct gain modulation by stimulated Raman scattering. We believe this new bandwidth enhancement mechanism may have important applications in optical communication and signal processing.

©2010 Optical Society of America

OCIS codes: (140.5960) Semiconductor lasers; (190.5650) Raman effect; (250.5590) quantum-well, -wire and -dot devices.

References and links

1. R. H. Wang, A. Stintz, P. M. Varangis, T. C. Newell, L. F. Lester, and K. J. Malloy, "Room-temperature operation of InAs quantum-dash lasers on InP (001)," IEEE Photon. Technol. Lett. **13**(8), 767–769 (2001).
2. D. Zhou, R. Piron, M. Dontabactouny, O. Dehaese, F. Grillot, T. Batte, K. Tavernier, J. Even, and S. Loualiche, "Low-threshold current density InAs quantum dash lasers on InP (100) grown by molecular beam epitaxy," Electron. Lett. **45**(1), 50–51 (2009).
3. R. Schwertberger, D. Gold, J. P. Reithmaier, and A. Forchel, "Long-wavelength InP-based quantum-dash lasers," IEEE Photon. Technol. Lett. **14**(6), 735–737 (2002).
4. B. S. Ooi, H. S. Djie, Y. Wang, C. L. Tan, J. C. M. Hwang, X. M. Fang, J. M. Fastenau, A. W. K. Liu, G. T. Dang, and W. H. Chang, "Quantum dashes on InP substrate for broadband emitter applications," IEEE J. Sel. Top. Quantum Electron. **14**(4), 1230–1238 (2008).
5. S. Azouigui, B. Dagens, F. Lelarge, J. G. Provost, D. Make, O. Le Gouezigou, A. Accard, A. Martinez, K. Merghem, F. Grillot, O. Dehaese, R. Piron, S. Loualiche, Z. Qin, and A. Ramdane, "Optical Feedback Tolerance of Quantum-Dot- and Quantum-Dash-Based Semiconductor Lasers Operating at 1.55 µm," IEEE J. Sel. Top. Quantum Electron. **15**, 764–773 (2009).
6. F. Lelarge, B. Dagens, J. Renaudier, R. Brenot, A. Accard, F. Dijk, D. Make, O. L. Gouezigou, J.-G. Provost, F. Poingt, J. Landreau, O. Drisse, E. Derouin, B. Rousseau, F. Pommereau, and G.-H. Duan, "Recent Advances on InAs/InP Quantum Dash Based Semiconductor Lasers and Optical Amplifiers Operating at 1.55 µm," IEEE J. Sel. Top. Quantum Electron. **13**(1), 111–124 (2007).
7. B. Dagens, D. Make, F. Lelarge, B. Rousseau, M. Calligaro, M. Carbonnelle, F. Pommereau, A. Accard, F. Poingt, L. Le Gouezigou, C. Dernazaretian, O. Le Gouezigou, J. G. Provost, F. van Dijk, P. Resneau, M. Krakowski, and G. H. Duan, "High Bandwidth Operation of Directly Modulated Laser Based on Quantum-Dash InAs-InP Material at 1.55 µm," IEEE Photon. Technol. Lett. **20**(11), 903–905 (2008).
8. Z. Mi, and P. Bhattacharya, "DC and dynamic characteristics of P-doped and tunnel injection 1.65-µm InAs quantum-dash lasers grown on InP (001)," IEEE J. Quantum Electron. **42**, 1224–1232 (2006).
9. H. S. Djie, C. L. Tan, B. S. Ooi, J. C. M. Hwang, X.-M. Fang, Y. Wu, J. M. Fastenau, W. K. Liu, G. T. Dang, and W. H. Chang, "Ultra-broad stimulated emission from quantum-dash laser," Appl. Phys. Lett. **91**(11), 111116 (2007).
10. B. S. Ooi, T. K. Ong, and O. Gunawan, "Multiple-wavelength integration in InGaAs–InGaAsP structures using pulsed laser irradiation-induced quantum-well intermixing," IEEE J. Quantum Electron. **40**(5), 481–490 (2004).
11. N. Naderi, M. Pochet, F. Grillot, N. Terry, V. Kovanis, and L. F. Lester, "Modeling the Injection-Locked Behavior of a Quantum Dash Semiconductor Laser," IEEE J. Sel. Top. Quantum Electron. **5**, 563–571 (2009).
12. C. Chen, S. Halder, B. S. Ooi, and J. C. M. Hwang, "Intrinsic response of quantum dash lasers under optical modulation," Proc. IEEE Lasers Electro-optical Soc. Annual Meet., 471–472 (2008).

#122035 - $15.00 USD Received 4 Jan 2010; revised 25 Feb 2010; accepted 4 Mar 2010; published 12 Mar 2010

13. C. B. Su, J. Eom, C. H. Lange, C. B. Kim, R. B. Lauer, W. C. Rideout, and J. S. Lacourse, "Characterization of the dynamics of semiconductor-lasers using optical modulation," IEEE J. Quantum Electron. **28**(1), 118–127 (1992).
14. T. Keating, X. Jin, S. L. Chuang, and K. Hess, "Temperature dependence of electrical and optical modulation responses of quantum-well lasers," IEEE J. Quantum Electron. **35**(10), 1526–1534 (1999).
15. L. Sirleto, M. A. Ferrara, I. Rendina, S. N. Basu, J. Warga, R. Li, and L. D. Negro, "Enhanced stimulated Raman scattering in silicon nanocrystals embedded in silicon-rich nitride/silicon superlattice structures," Appl. Phys. Lett. **93**(25), 251104 (2008).
16. J. Hu, B. S. Marks, and C. R. Menyuk, "Flat-gain fiber Raman amplifiers using equally spaced pumps," J. Lightwave Technol. **22**(6), 1519–1522 (2004).
17. C. Chen, Y. Wang, C. L. Tan, H. S. Djie, B. S. Ooi, J. C. M. Hwang, G. T. Dang, and W. H. Chang, "Effects of Intermixing on Gain and Alpha Factors of Quantum-Dash Lasers," IEEE Photon. Technol. Lett. **20**(19), 1654–1656 (2008).
18. T. Tanabe, K. Suto, T. Saito, T. Kimura, Y. Oyama, and J. Nishizawa, "Characteristics of time-gated Raman amplification in GaP–AlGaP semiconductor waveguides," Appl. Phys. Lett. **93**, 43–45 (2003).
19. R. Claps, D. Dimitropoulos, V. Raghunathan, Y. Han, and B. Jalali, "Observation of stimulated Raman amplification in silicon waveguides," Opt. Express **11**(15), 1731–1739 (2003).

1. Introduction

Quantum-dash lasers [1] have been intensively studied for their unique characteristics, including low threshold current [2], wide temperature range [3], broadband emission [4], feedback insensitivity [5], low noise [6], and distinctive modulation behavior [7,8]. In this paper, we report another unique characteristic in terms of sharply enhanced modulation bandwidth in InAs/InAlGaAs/InP quantum-dash lasers under optical injection modulation when the injection wavelength is 65 ± 5 nm shorter than the lasing wavelength. Based on rate equation models, we postulate that the bandwidth is enhanced by stimulated Raman scattering, which, to our knowledge, has not previously been reported as a modulation mechanism for semiconductor lasers.

2. Laser structure and experimental setup

Table 1. Types of Lasers Tested

Type	I	II	III
Heterostructure	InGaAs/InGaAsP/InP	InAs/InAlGaAs/InP	
Active Material	Well	Dash	
Number of Layers	5	4	5
Density	—	10^{10} cm^{-2}	
Size	5.5 nm	(20-75) × 18 × 3 nm^3	300 × 25 × 5 nm^3
Cavity Length	400 μm	400 μm	450 μm
Ridge Width	3 μm	3 μm	4 μm
Threshold Current	22 mA	215 mA	46 mA
Emission Wavelength	1600 nm	1620 nm	1565 nm
Emission Bandwidth	<10 nm	>10 nm	~10 nm
Modulation Efficiency	0.97 GHz/mA^{½}	0.36 GHz/mA^{½}	0.55 GHz/mA^{½}
K Factor	0.28 ns	0.81 ns	0.31 ns
Reference	[10]	[4]	[11]

Table 1 lists the three types of lasers tested, all with cleaved and unpassivated facets. The first is a quantum-well laser [10]; the second and third are quantum-dash lasers. Due to subtle differences in fabrication, the two quantum-dash lasers differ in emission wavelength and other characteristics. In particular, the 1620-nm laser [4,9] has less uniform dashes, higher threshold current, and broader emission width than the 1565-nm laser [11].

All three types of lasers are tested by using a custom setup [12] for optical injection modulation. Unlike in *optical injection locking*, in *optical injection modulation* the laser-under-test is electrically biased into lasing but the modulation is accomplished by using an optical modulator between the laser-under-test and the injection laser. This helps reveal the intrinsic characteristics of the laser-under-test without being hindered by parasitic resistances and capacitances [13]. The self-heating effect is also minimized by sub-microsecond pulsing of both the electrical bias and the optical injection, which is a unique capability of the custom

#122035 - $15.00 USD Received 4 Jan 2010; revised 25 Feb 2010; accepted 4 Mar 2010; published 12 Mar 2010
(C) 2010 OSA

setup. The pulsed optical injection is in turn modulated by a $LiNbO_3$ Mach-Zehnder modulator driven by the amplified signals of a time-gated microwave network analyzer between 0.5 and 10 GHz. All modulation responses are normalized by their values at 0.5 GHz to eliminate the uncertainty due to variations in coupling efficiency. The source for optical injection can be either a narrowband laser at 1310 nm or a tunable laser between 1460 nm and 1580 nm. All tests are performed on bare laser chips at 20°C in dry air.

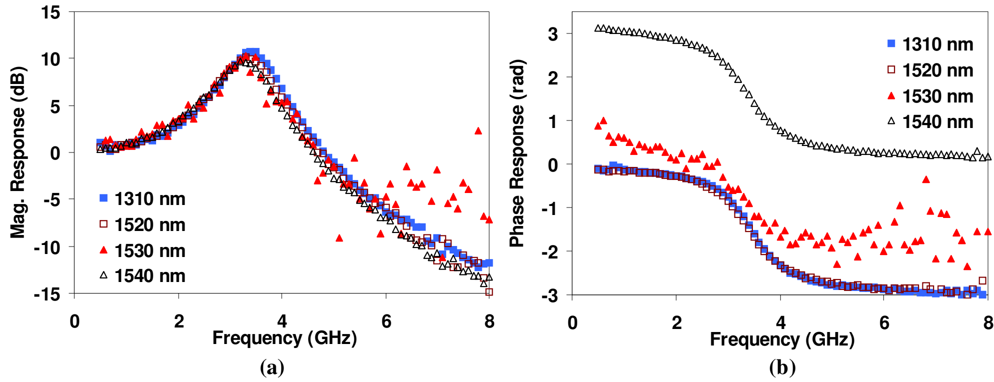

Fig. 1. Measured (a) magnitude and (b) phase of the response of a 1600-nm *quantum-well* laser biased with 33 mA and optical injection modulated with different injection wavelengths and modulation frequencies.

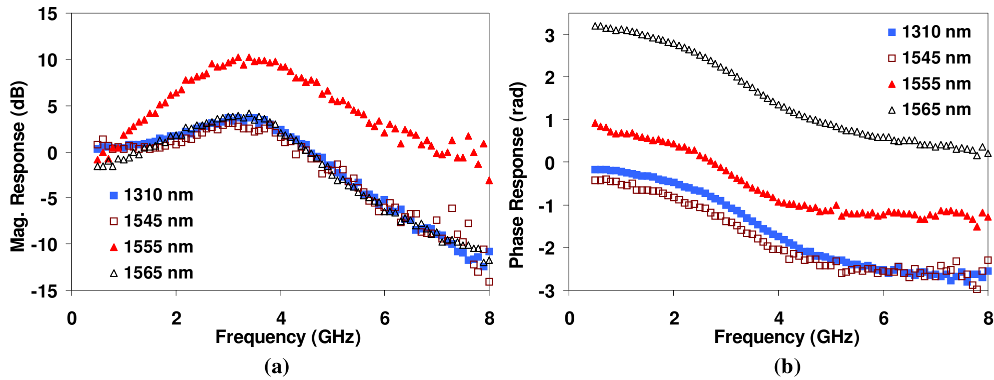

Fig. 2. Measured (a) magnitude and (b) phase of the response of a 1620-nm *quantum-dash* laser biased with 298 mA and optical injection modulated with different injection wavelengths and modulation frequencies.

#122035 - $15.00 USD Received 4 Jan 2010; revised 25 Feb 2010; accepted 4 Mar 2010; published 12 Mar 2010
(C) 2010 OSA

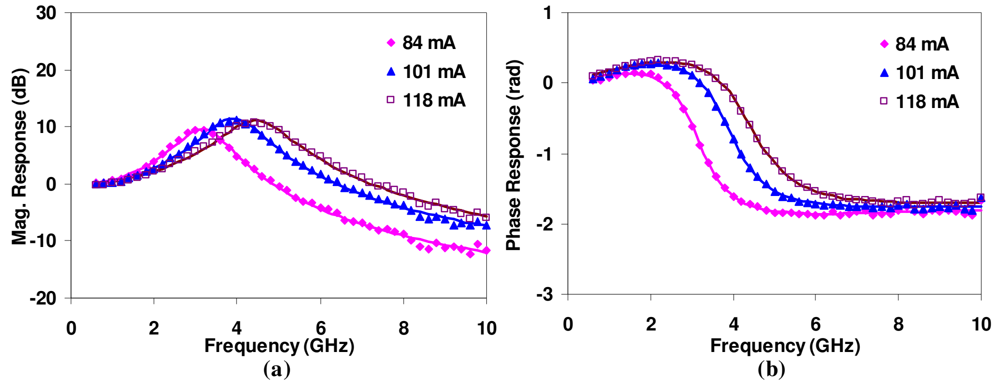

Fig. 3. Measured (symbol) vs. modeled (curve) (a) magnitude and (b) phase response vs. frequency of a 1565-nm *quantum-dash* laser electrically biased at different currents and optical injection modulated at *1490 nm*.

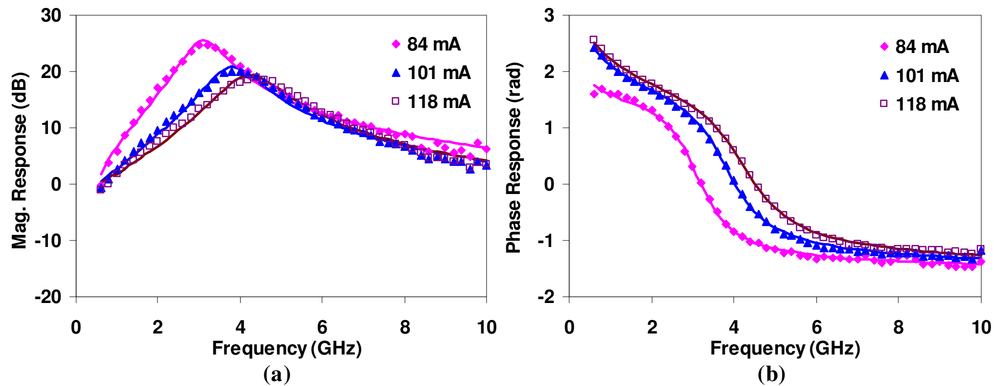

Fig. 4. Measured (symbol) vs. modeled (curve) (a) magnitude and (b) phase response vs. frequency of a 1565-nm *quantum-dash* laser electrically biased at different currents and optical injection modulated at *1500 nm*.

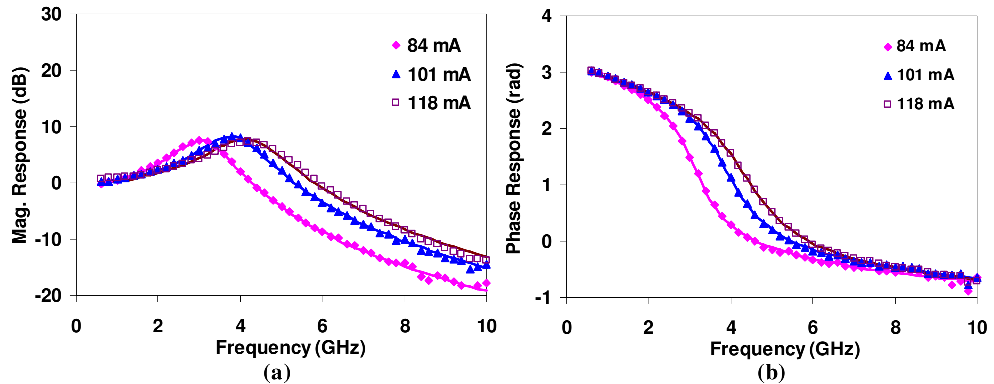

Fig. 5. Measured (symbol) vs. modeled (curve) (a) magnitude and (b) phase response vs. frequency of a 1565-nm *quantum-dash* laser electrically biased at different currents and optical injection modulated at *1510 nm*.

#122035 - $15.00 USD Received 4 Jan 2010; revised 25 Feb 2010; accepted 4 Mar 2010; published 12 Mar 2010
(C) 2010 OSA

3. Effects of optical injection wavelength and microwave modulation frequency

Figure 1 shows the classical [14] frequency response to optical injection modulation measured on the *quantum-well* laser. Both the magnitude and phase of the response are conveniently recorded by the microwave network analyzer, which corrects for the loss and delay of cables and connectors after a standard calibration procedure. It can be seen that the response patterns are similar between different injection wavelengths. However, at 1530 nm when the laser transitions between gain and absorption, the response is ~20 dB weaker and the data are much noisier. As the signal intensity is affected by variations in coupling efficiency, presently the absolute change in modulation efficiency cannot be more accurately assessed. The phase of the response changes by π as in any resonance phenomena. The phase response will be discussed in detail at the end of Sec. 4.

By contrast, the response measured on the two *quantum-dash* lasers near the gain-absorption transition is stronger and more broadband than at other injection wavelengths. Figure 2 shows the response of the 1620-nm quantum-dash laser. It can be seen that the bandwidth is significantly enhanced at the injection wavelength of 1555 nm. However, just 10 nm off, at 1545 nm or 1565 nm, the response is as classical as that at 1310 nm. Figures 3-5 show similar bandwidth enhancement of the 1565-nm quantum-dash laser, although its many other characteristics are different from that of the 1620-nm quantum-dash laser. It can be seen that the response at 1500 nm is qualitative different from that at 1490 nm or 1510 nm, independent of the bias current. In spite of the different lasing wavelengths of the two quantum-dash lasers, bandwidth enhancement always occurs when the injection wavelength is 65 ± 5 nm below the lasing wavelength. In either case, the bandwidth enhancement effect does not change significantly if the optical injection power is varied from 0.6 mW to 1.2 mW. The maximum power is limited by the output of the injection laser; the minimum power is limited by the signal-to-noise ratio.

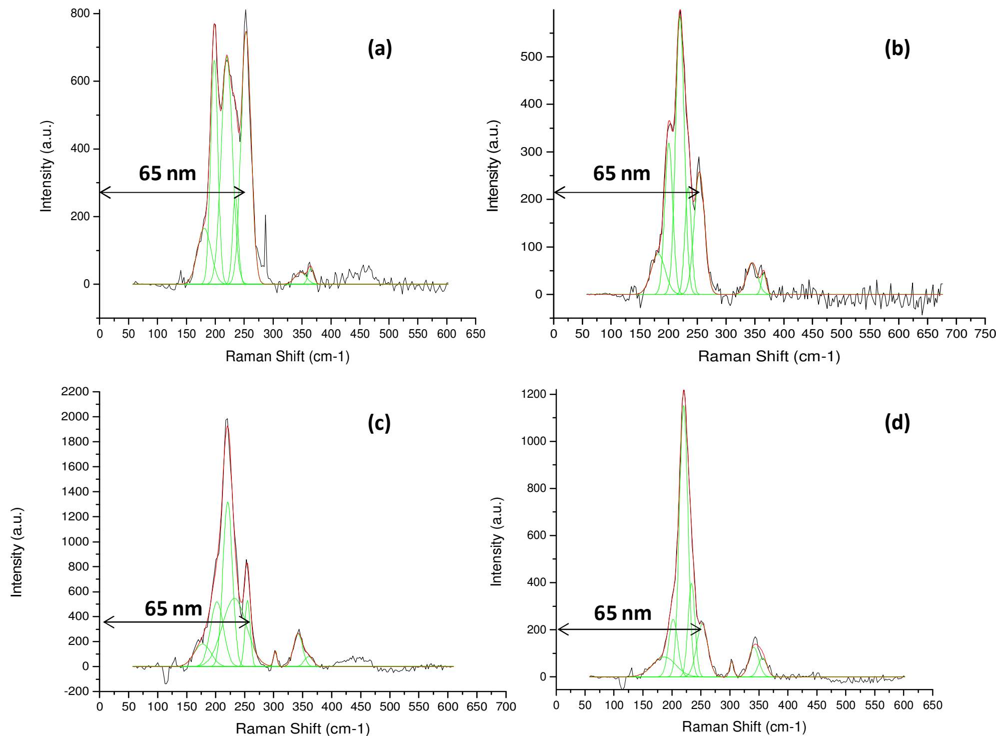

Fig. 6. Measured (a) z(yy)z, (b) z(xy)z, (c) z(yx)z and (d) z(xx)z Raman shift of a quantum-dash structure similar to that of the 1620-nm laser.

#122035 - $15.00 USD Received 4 Jan 2010; revised 25 Feb 2010; accepted 4 Mar 2010; published 12 Mar 2010
(C) 2010 OSA

4. Rate equation model

Figure 6 shows that the above-described difference of 65 ± 5 nm coincides with the Raman shift we measured on a quantum-dash structure similar to that of the 1620-nm quantum-dash laser. The measured InAs LO phonons are in the range of 252-260 cm^{-1}, which corresponds to a wavelength of 63-66 nm. Therefore, we postulate that due to the strong stimulated emission around the lasing wavelength, an injection at the right wavelength can stimulate Raman scattering in the laser cavity and be coupled into the lasing mode. This can explain the strong response when the emission and injection wavelengths differ by the Raman shift. However, the difference in the frequency response pattern requires more detailed explanation by using rate equation models.

The frequency response of a quantum-well laser to optical injection modulation can be expressed as [14]

$$M = \frac{\alpha \Gamma v \tau_P f_R^{\,2}}{f_R^{\,2} - f^2 + j\gamma f / 2\pi} \tag{1}$$

where f is the modulation frequency, α is the absorption coefficient, Γ is the optical confinement factor, v is the group velocity, τ_P is the photon lifetime, f_R is the relaxation frequency, and γ is the damping factor. Equation (1) can be modified to include stimulated Raman scattering by considering the following rate equations

$$\frac{dN_W}{dt} = \frac{\eta I}{qV_W} - \frac{N_W}{\tau_C} - \frac{N_W}{\tau_W} + \frac{N_D}{\delta \tau_E} \tag{2}$$

$$\frac{dN_D}{dt} = \frac{\delta N_W}{\tau_C} - \frac{N_D}{\tau_E} - \frac{N_D}{\tau_D} - \frac{v(G + g\Delta N_D)S}{1 + \varepsilon S} + \alpha v S_I \tag{3}$$

$$\frac{dS}{dt} = \frac{\Gamma v(G + g\Delta N_D)S}{1 + \varepsilon S} - \frac{S}{\tau_P} + \psi S_I S \tag{4}$$

where q is the electron charge, N_W and N_D are carrier densities in quantum wells and dashes, ΔN_D is the small-signal variation of N_D, S and S_I are photon densities of laser emission and optical injection, I is the bias current, η is the current injection efficiency, δ is the volume ratio between quantum wells and dashes, τ_C and τ_E are carrier capture and escape times, τ_W and τ_D are carrier lifetimes in quantum wells and dashes, ε is the gain compression factor, and G and g are static and differential gains, respectively. The last term in Eq. (3) represents optical injection modulation; the last term in Eq. (4) reprsents stimulated Raman scaterring, with ψ being the coupling coefficient. Both α and ψ are functions of the injection wavelength. Spontaneous emission is omitted in Eq. (4) because its impact is negligible under the present circumstances.

The small-signal solution of Eqs. (2)-(4) is

$$M' = \frac{\left[\alpha \Gamma v \tau_P + \psi S_0 \left(\tau_P + 1/4\pi^2 \tau_D' f_R^2\right)\right] f_R^2}{f_R^2 - f^2 + j\gamma f / 2\pi} (1 + j2\pi \tau_R f) \tag{5}$$

$$1/\tau_R = 1/\tau_D' + 4\pi^2 \tau_P f_R^2 \left(1 + \alpha \Gamma v / \psi S_0\right) \tag{6}$$

$$f_R^{\,2} = \frac{vg' S_0}{4\pi^2 \tau_P (1 + \varepsilon S_0)} \left(1 + \frac{\varepsilon}{vg' \tau_D'}\right) - \frac{\psi S_{I0}}{4\pi^2} \left(\frac{1}{\tau_D'} + \frac{vg' S_0}{1 + \varepsilon S_0}\right) \tag{7}$$

$$\gamma = \frac{1}{\tau_D'} + \frac{vg' S_0}{1 + \varepsilon S_0} + \frac{\varepsilon S_0}{\tau_P (1 + \varepsilon S_0)} - \psi S_{I0} \tag{8}$$

#122035 - $15.00 USD Received 4 Jan 2010; revised 25 Feb 2010; accepted 4 Mar 2010; published 12 Mar 2010
(C) 2010 OSA

where $\tau'_D = \tau_D (1 + \tau_C / \tau_E)$ is the effective carrier lifetime in quantum dashes, $g' = g (1 + \tau_C / \tau_E)$ is the effective differential gain, S_0 and S_{I0} are static photon densities of laser emission and optical injection, respectively, and τ_R is a bandwidth enhancement factor due to stimulated Raman scattering.

Comparing Eq. (5) to Eq. (1), M' differs from M in frequency response mainly due to the additional term of $1 + j2\pi\tau_R f$, which changes the high-frequency dependence from $1/f^2$ to $1/f$. This is consistent with the change from 12 dB/octave to 6 dB/octave in the high-frequency rolloff of the measured response magnitude $M'M'^*$ shown in Fig. 2(a). Further, by adjusting τ_R through its dependence on the the Raman coupling coefficient ψ according to Eq. (6), the frequency response of M' can match the measured data under different bias currents and injection wavelengths as shown in Figs. 3-5. Thus, by adding only one parameter ψ for stimulated Ramance scattering, M' can efficiently fit the new frequency response pattern. On the other hand, if $\psi = 0$, then $M' = M$.

Equation (1) describes the resonance of the modulation frequency f around the relaxation frequency f_R in the 1600-nm quantum-well laser with its phase response θ illustrated in Fig. 1(b). For the absorption at the injection wavelength of 1540 nm, $\alpha < 0$ so that $\theta \approx \pi$ when $f << f_R$ and $\theta \approx 0$ when $f >> f_R$. With gain at 1310 nm and 1520 nm, $\alpha > 0$ so that $\theta \approx 0$ when $f << f_R$ and $\theta \approx -\pi$ when $f >> f_R$. For the gain-absorption transition at 1530 nm, $\alpha \approx 0$ so that $0 < \theta < \pi$ when $f << f_R$ and $-\pi < \theta < 0$ when $f >> f_R$. With stimulated Raman scattering in the quantum-dash lasers, Eq. (5) is more complicated than Eq. (1), but the general trend of the phase response is similar as shown in Fig. 2(b)-Fig. 5(b).

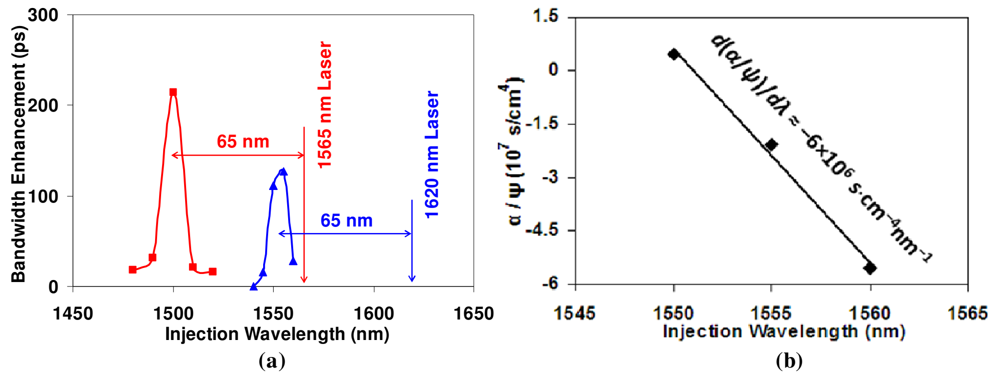

Fig. 7. (a) Bandwidth enhancement factor $|\tau_R|$ and (b) injection-to-Raman gain ratio α/ψ as functions of the injection wavelength extracted on quantum-dash lasers.

5. Discussion

Figure 7(a) shows that the extracted bandwidth enhancement factor τ_R peaks at 100-200 ps in a spectral window of ~10 nm around the injection wavelengths of 1500 nm and 1560 nm for the 1565-nm and 1620-nm quantum-dash laser structures, respectively. This enhancement is dependent on both the injection gain (or absorption) and the Raman gain. Because the laser emission from quantum dashes has a broad spectrum [4] and the Raman gain in low-dimensional structures may be inherently broader than in bulk materials [15], this relatively broad spectral window for enhancement is not surprising.

The aforementioned characteristics can be used to estimate the value of Raman gain required to produce the observed modulation bandwidth enhancement. For the present modulation frequency range of 10 GHz, the last term of Eq. (5) is significant only when τ_R peaks. According to Eq. (6), τ_R is proportional to ψ/α, with ψ and α both varying with the injection wavelength. Therefore, a large ψ is insufficient for the modulation bandwidth to be enhanced by stimulated Raman scattering; large ψ and small α must occur at the same injection wavelength. However, although it appears to occur in the two different types of

quantum-dash lasers tested, it may not occur in *all* quantum-dash lasers. More quantum-dash lasers need to be investigated to see whether or not *all* quantum-dash lasers exhibit such a bandwidth enhancement effect. In the case of the 1600-nm qunatum-well laser, the modulation response is ~20 dB weaker at 1530 nm, which indicates that the gain-absorption transiton occurs around 65-nm detuning with a small α there. However, since no bandwidth enhancement is observed, ψ must be small around 65-nm detuning. There may still be Raman scattering in the quantum-well laser, but it may be overwhelmed by gain or absorption modulation.

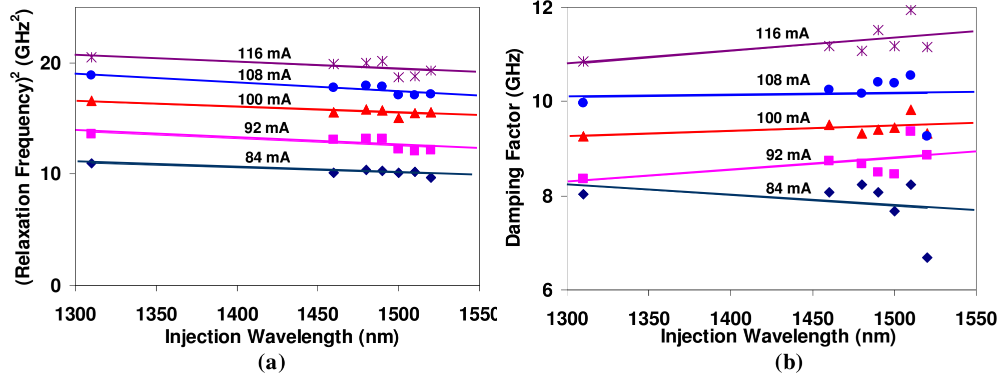

Fig. 8. Extracted (a) relaxation frequency f_R^2 and (b) damping factor γ of a 1565-nm quantum-dash laser biased with different currents and optical injection modulated with different wavelengths.

Comparing to classical expressions [14], Eqs. (8) and (9) show that both the relaxation frequency f_R and the damping factor γ contain an additional term that is dependent on ψ. However, Fig. 8 shows that the f_R and γ values extracted from the 1565-nm quantum-dash laser are only weakly dependent on the injecion wavelength. This confirms that the sharp wavelength dependence of bandwith enhancement is mainly due to the last term of Eq. (5).

The injection-to-Raman gain ratio α/ψ can be calculated according to Eq. (6) by using the τ_R values extracted earlier on the 1620-nm laser and estimated parameter values such as τ'_D = 0.17 ns, τ_P = 2.8 ps, Γ = 0.015 and $S_0 \approx 3 \times 10^{14}$ cm^{-3}. Figure 7(b) shows the calculated wavelength dependence of α/ψ has a slope of $d(\alpha/\psi)/d\lambda = -6 \times 10^6$ s·cm^{-4}nm^{-1}. From this value the stimulated Raman gain g_R can in turn be estimated by considering the following alternative to Eq. (4) [16]

$$\frac{dP}{dz} = G_P P + \frac{g_R}{2A} P P_I \tag{9}$$

where P and P_I are optical powers of the laser emission and optical injection, respectively, G_P is the net gain of the laser power, and A is the effective area of the laser waveguide. The last terms of Eq. (4) and Eq. (9) are equal because they both describe the stimulated Raman scattering. Therefore,

$$\psi S_I = \frac{v g_R P_I}{2A} = \frac{g_R v^2 hc}{2\lambda} S_I \tag{10}$$

where h is Plank's constant, c is the speed of light, and λ is the injection wavelength. Thus,

$$\psi = \frac{g_R v^2 hc}{2\lambda}. \tag{11}$$

Within the 10-nm region of the transition from gain to absorption for the injected signal, the effective g_R for the Raman term in the rate equations can be assumed to be constant due to broadband laser emission and high-degree quantum confinement. In comparison, near the gain-absorption transition wavelength λ_T, the absorption coefficient α can be assumed to depend linearly on λ

$$\alpha = B(\lambda_T - \lambda) \tag{12}$$

where $B \approx 40$ cm^{-1}/nm according to the gain spectrum [17] measured on the same laser. Thus,

$$\frac{\alpha}{\psi} = \frac{2B\lambda(\lambda_T - \lambda)}{g_R v^2 hc} \tag{13}$$

and

$$\frac{d\left(\alpha/\psi\right)}{d\lambda} \approx \frac{2B(\lambda_T - 2\lambda)}{g_R v^2 hc}. \tag{14}$$

For $\lambda = \lambda_T$

$$g_R = -\frac{2B\lambda_T}{v^2 hc} \Bigg/ \left.\frac{d(\alpha/\psi)}{d\lambda}\right|_{\lambda=\lambda_T}. \tag{15}$$

Using Eq. (15), the Raman gain coefficient g_R is estimated to be on the order of 10^{-8} m/W. This value for InAs quantum dashes is a little higher than the stimulated Raman gain for bulk GaP waveguides [18], possibly due to better quantum confinement as has been observed in silicon nanocrystals [15]. This value is also much higher than that for silicon waveguides [19].

6. Conclusion

A new bandwidth enhancement mechanism was observed in quantum-dash lasers under optical injection modulation when the injected photons are 33 ± 3 meV more energetic than the lasing photons. Based on rate equation models, the new mechanism was attributed to the coincidence of strong stimulated Raman scattering and weak absorption at the same injection wavelength in highly confined quantum structures. The coincidence of stimulated Raman scattering and weak absorption sharply enhanced the modulation bandwidth by changing the high-frequency roll-off pattern from $1/f^4$ to $1/f^2$. The stimulated Raman gain for the present InAs quantum dashes was estimated to be on the order of 10^{-8} m/W, which is higher than that for either GaP or silicon waveguides. Such a strong stimulated Raman gain may have important applications in optical communication and signal processing.

Acknowledgement

This work was supported in part by a subcontract from Alcatel-Lucent Bell Laboratories under the DOD-N IRIS program of the Defense Advanced Projects Agency of the USA, and a grant (No. 0725647) from the National Science Foundation of the USA.